Oscillatory failure detection in the flight control system of a civil aircraft using soft sensors*

Do Hieu Trinh†, Benoît Marx†, Philippe Goupil‡ and José Ragot†

Abstract. This chapter aims to detect oscillatory failures affecting a flight control surface (FCS) -specifically an aileron- of an aircraft. It presents the principle of supervision and the design of a soft sensor for the oscillatory failure case detection. The chosen principle for diagnosis is based on testing the adequacy of available measures in a control system (CS) servo-loop toward its model. Two kinds of failures must be detected, which are identified as "liquid failure" and "solid failure" as a disturbing signal is superimposed on or replaces the control signal. The chapter tackles the problem of fault detection and isolation (FDI) by the test of standard deviation. This problem is treated by a correlation test between several residuals. The quantitative analysis of residues confirms visual study and shows how the recognition is automatically processed from a numerical point of view.

Keywords. Soft sensor, fault detection and isolation, oscillatory failure, flight control surface, civil aircraft, correlation test, standard deviation test.

1 Introduction

The safe operation of a physical process can be harmed on the occurrence of faults, these faults may affect the process itself or its conduct bodies. This observation has naturally led to the implementation of surveillance systems whose objective is to be able at any moment, to provide operating status of the various organs constituting the system. When a fault occurs, it must be detected as soon as possible, even where all observed signals remain in their allowable limits. It must then be located and its cause identified. Thus, the steps of observation and monitoring must be assisted by a "smarter" step.

This step, called supervision, uses all available information through an implicit or explicit model. Here, the goal is the detection of oscillatory failures affecting a flight control system (FCS) -specifically an aileron- of an aircraft.

*How to cite this chapter. Trinh, D. H., Marx, B., Goupil, P. and Ragot, J. (2014) Oscillatory Failure Detection in the Flight Control System of a Civil Aircraft Using Soft Sensors, Chap. 5 in *New Sensors and Processing Chain* (eds J.-H. Thomas and N. Yaakoubi), John Wiley & Sons, Inc., Hoboken, NJ, USA.

†Université de Lorraine, CRAN UMR 7039, 2, avenue de la forêt de Haye, Vandoeuvre-lès-Nancy, Cedex 54516, France and CNRS, CRAN, UMR 7039, France.

‡EDYC-CC Flight Control System, AIRBUS Operations S.A.S

For these oscillatory failures, airworthiness regulations applied worldwide by all manufacturers require precaution designed to detect and to accommodate these failures [5, 10]. Software embedded on the Airbus A380, for example, is entirely compliant to the current regulations. However, improvements [9] could be used for the next generation of aircraft from European manufacturer to accompany the future technological innovations and meet changing regulations. That is the purpose of this study. Examples of oscillatory failures detection in other areas can be found in [3, 6]. Note also that these oscillatory failures are different from Pilot-Induced Oscillations (PIO) caused by the pilot [7, 11]. In the following, some elements leading to a methodology to detect such failures are presented, which are based on existing sensors and on *soft (or virtual) sensors* capable of reconstructing some informations through a model of the sensors.

The principle of supervision is presented in the section 2 and the design of a soft sensor for the oscillatory failure case detection in the section 3. The section 4 tackled the problem of fault detection and isolation (FDI) by the test of standard deviation. This problem is treated in the section 5 by a test of correlation between several residuals. Conclusion and perspectives end the paper.

2 Modeling of studied system

The traditional approach to detecting and isolating faults in a flight control system makes use of hardware redundancy by a replication of hardware [5] such as sensors, actuators or even flight control computers [13]. However, in respect to financial cost, there is a growing interest in methods which do not require additional hardware redundancy, these methods being based on software redundancy [1, 15, 12, 2].

Fault diagnosis methods are generally classified into two groups, model-based and data-driven methods depending on the knowledge we have or not on the system under investigation. Here we are involved with a relatively simple system that can be modeled easily from mechanical considerations and physical assumptions.

The chosen principle for diagnosis is based on testing the adequacy of available measures in a CS servo-loop towards its model. Thus, it is necessary to establish the model of the system, generating through this model and the available measures an indicator of failure. This indicator must be analyzed to detect the presence of this failure as soon as possible. A model called *failure-free* can be proposed simulating the system behavior in the absence of failure. *Failure models* corresponding to system behaviors in occurrence of oscillations can also be established. Two kinds of failures must be detected, which are identified as "liquid failure" and "solid failure" as a disturbing signal is superimposed on or replaces the control signal [9, 14]. The probable sources of oscillatory failure are presented in figure 1.

In this application, the characteristic variables of CS servo-loop are given in the table 1.

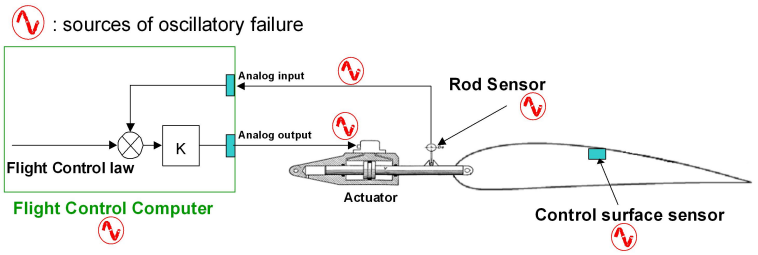

Figure 1: The probable sources of oscillatory failure

$x_b(t)$	position of the rod of CS actuator (aileron)
$u(t)$	position's order of CS actuator
$F_a(t)$	aerodynamic forces applied on the CS
$M_a(t)$	aerodynamic force moment
$\Delta P(t)$	difference of hydraulic pressure in the input of the FCS actuator
$V_0(t)$	speed computed by flight control computer
$x(t)$	position (in degrees) of the CS
$K_a(t)$	damping coefficient of adjacent actuator (case of 2 actuators per CS)
ΔP_{ref}	pressure of reference
τ	transmission delay of the sensor
S	surface area of the actuator's piston
K	control gain

Table 1: Characteristic variables and constants of CS servo-loop

The failure-free model M_b is described structurally as follows:

$$M_b = \begin{cases} \dot{x}_b(t) &= V_0(t)\sqrt{\dfrac{S\Delta P(t) + \text{sign}(V_0(t))F_a(t)}{S\Delta P_{ref} + K_a(t)V_0^2(t)}} \\ V_0(t) &= K(u(t) - x_b(t-\tau)) \\ \Delta P(t) &= f_1(x_d(t)) \\ K_a(t) &= f_2(x_d(t)) \\ F_a(t) &= f_3(M_a(t), x_d(t)) \\ x(t) &= f_4(x_b(t), \tau) \end{cases} \quad (1)$$

where the structure of functions $f_i(.)$ are not detailed here. The quantities $\Delta P(t)$, $K_a(t)$ and $F_a(t)$, generally unmeasurable, play the role of disturbance of which one can know the domain of variation. Failure models of solid and liquid types take the following forms respectively:

$$M_s = \begin{cases} \dot{x}_s(t) &= V_{0,s}(t)\sqrt{\dfrac{S\Delta P(t) + \text{sign}(V_{0,s}(t))F_a(t)}{S\Delta P_{ref} + K_a(t)V_{0,s}^2(t)}} \\ V_{0,s}(t) &= S_{def,s}(t) \end{cases} \quad (2)$$

$$M_\ell = \begin{cases} \dot{x}_\ell(t) & = & V_{0,l}(t)\sqrt{\dfrac{S\Delta P(t) + \text{sign}(V_{0,\ell}(t))F_a(t)}{S\Delta P_{ref} + K_a(t)V_{0,\ell}^2(t)}} \\ V_{0,\ell}(t) & = & K(u(t) - x_\ell(t-\tau)) + S_{def,\ell}(t) \end{cases} \quad (3)$$

where the magnitudes of $\Delta P(t)$, $K_a(t)$ and $F_a(t)$ depend on flight scenario; $S_{def}(t)$ represents the oscillatory failure signal of unknown frequency, but characterized by a known frequency range (from 0.5 Hz to 12 Hz). It is important to note that the two models M_b, M_s are related to the failure of a non-linear way. That will explain the further comments in section about the frequency of the failure 4.4).

The principle of supervision, which is therefore to determine at every moment, which mode of the system M_b, M_s or M_ℓ is active, is the subject of Section 3. Note that after recognition of a faulty mode, we have to define and apply a control signal allowing the reduction of the oscillations, but this is not the purpose of the current presentation, which is however addressed in some works [8].

3 Design of a soft sensor for the oscillatory failure detection

The evolution of outputs noted respectively x_b, x_s and x_ℓ are computed by integrating, according to the time, the equations related to the three modes of operation of CS. In this case, one speaks about soft sensor, because the simulation provides information comparable to what gives a physical sensor, under condition that the model is well representative of the system. At each time, this allows to propose a diagnostic strategy summarized in the table (2).

E_1	At time t, acquire the available measures
E_2	Evaluate the outputs ($x_b(t)$, $x_s(t)$, $x_\ell(t)$) of the three soft sensors
E_3	Calculate the residuals $r_\lambda(t) = x(t) - x_\lambda(t)$, $\lambda = b, s, \ell$
E_4	Compare the residuals $r_\lambda(t)$ in respect to given thresholds
E_5	Test of persistence over time of the result of statistic tests
E_6	Take the decision of the occurrence of a failure

Table 2: Strategy for Fault Detection

The comparison between the outputs of these soft sensors and the growths measured by physical sensors results in three residual signals allowing to determine the most representative model of the behavior of the CS and thus to determine the type of the potentially occurring failure. Note that one of the major difficulties in the implementation of this technique is due to the fact that the physical system is subjected to hardly measurable disturbances ($\Delta P(t)$, $K_a(t)$ and $F_a(t)$). In [9], the authors have shown that $\Delta P(t)$ and $F_a(t)$ cannot be

identified simultaneously and they have chosen to set $\Delta P(t)$ to its most likely value then identify $K_a(t)$ and $F_a(t)$. Taking into account the complexity of the estimation of $K_a(t)$ and $F_a(t)$ as well as the limited power of the flight control computer, the model was simplified by fixing the three perturbations $\Delta P(t)$, $K_a(t)$ and $F_a(t)$ with fixed nominal values ΔP_b, K_{ab} and F_{ab}[1]. From equation (1), the corresponding evolution of the output $x_b(t)$ is then reduced to:

$$M_b = \begin{cases} \dot{x}_b(t) = V_0(t)\sqrt{\dfrac{S\Delta P_b + \text{sign}(V_0(t))F_{ab}}{S\Delta P_{ref} + K_{ab}V_0^2(t)}} \\ V_0(t) = K(u(t) - x_b(t-\tau)) \end{cases} \tag{4}$$

In fact, there are several flight scenario (for example cruise phase, nose-up, triggering of pitch protection, yaw-angle-mode), and for each scenario the values of ΔP_b, K_{ab} and F_{ab} are adapted; this adaptation is not a handicap, because the recognition of the scenario is pretty obvious. Figure 2 shows the input of the system, the output of the nonlinear model (1) and that of its simplified model (4); the low amplitude of the difference between the two outputs fully justifies the use of simplified model (4). For this reason, constant values are

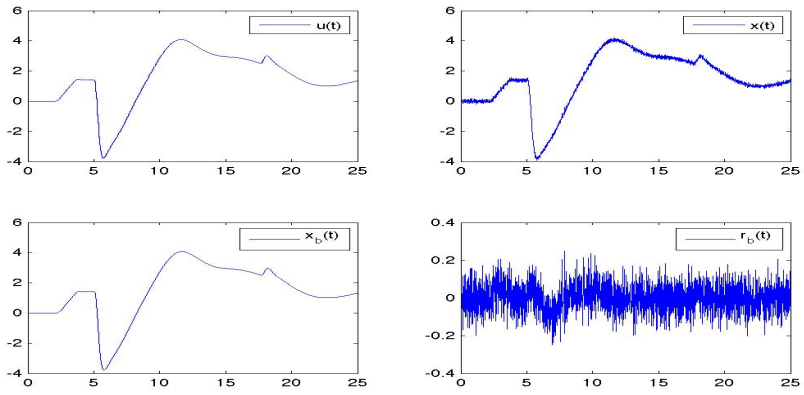

Figure 2: Validation of simplified model

also chosen for the perturbations in the solid and liquid failure models (2 and 3). In following the isolation of an oscillation of 0.5 degree amplitude and 1.5 Hz frequency will be considered. More generally, this case corresponds to an oscillatory failure signal $S_{def}(t)$ (for liquid and solid failures) described by:

$$S_{def}(t) = A \sin(2\pi f.t) \tag{5}$$

The whole FD procedure summarized in table 2 is applied, using the model of oscillatory failure signal (5) with the failure models (2 and 3), with a range of

[1]Numerical values of the system parameters are not given here for the sake of confidentiality

amplitude from 0.5 deg to 1 deg and a range of frequency from 0.5 Hz to 12 Hz (the sampling period for data acquisition is $0.01s$).

4 Fault detection by standard deviation test

4.1 Residual generation

With the actual measurement x of the CS position and outputs corresponding to the modes of operation of the system, three residuals are obtained from the simplified models M_b, M_s and M_ℓ as shown in figure 3. Figure 4, represents

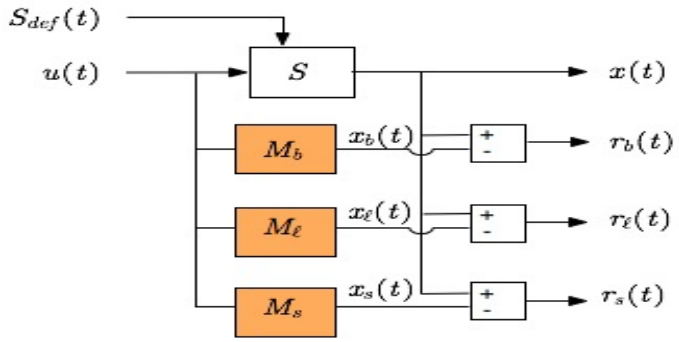

Figure 3: Bank of residues for the detection of failure

the residuals $r_b(t)$, $r_s(t)$ and $r_\ell(t)$ in the case without failure. In the absence of failure, model M_b really fits this situation, the amplitude of the residual $r_b(t)$ is clearly limited to approximately 0.2 deg; however, residuals $r_s(t)$ and $r_\ell(t)$ oscillate with a significantly greater amplitude that is justified by the fact that in absence of failure, model M_ℓ and M_s do not correspond to this situation.

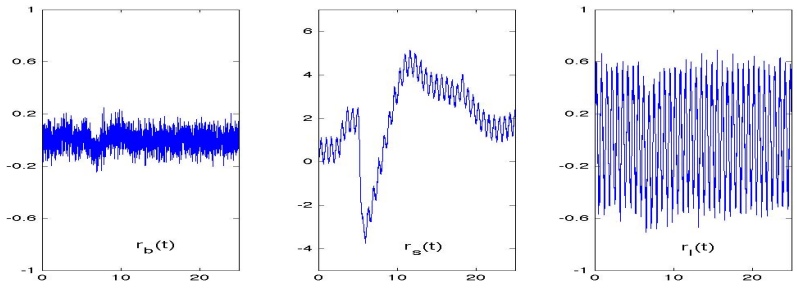

Figure 4: Residuals $r_b(t)$, $r_s(t)$ and $r_\ell(t)$: case without failure

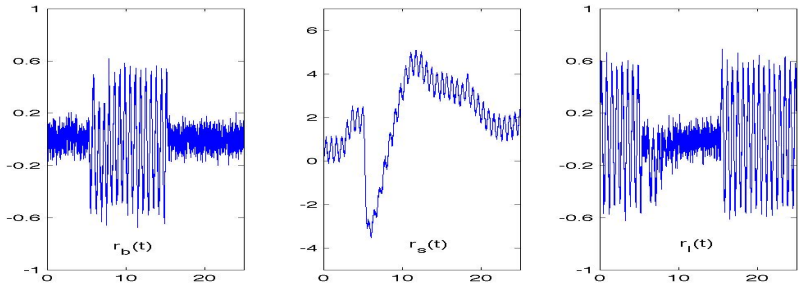

Figure 5: Residuals $r_b(t)$, $r_s(t)$ and $r_\ell(t)$: case of liquid failure

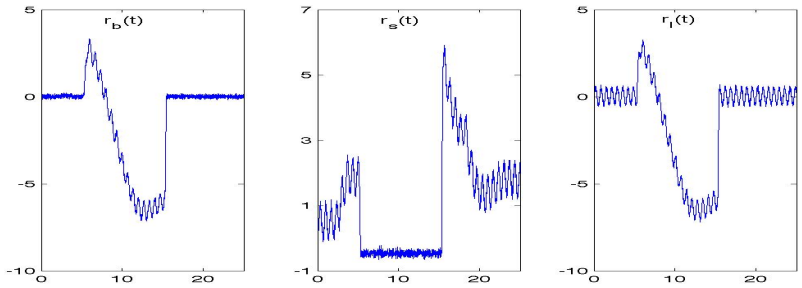

Figure 6: Residuals $r_b(t)$, $r_s(t)$ and $r_\ell(t)$: case of solid failure

Two other situations are now considered. Figure 5 (*resp.* figure 6) represents the residuals in the case of liquid failure (*resp.* solid failure). The failure is simulated between 5.3 s and 15.3 *s*. In this time interval, there is an increase of the variation of the residue $r_b(t)$ and a reduction in the variation of the residue $r_\ell(t)$ (*resp.* residue $r_s(t)$) in the presence of the liquid failure (*resp.* solid failure). These residues are used for the FDI procedure, the signatures of the residues being well differentiated according to the type of failure. Table 3 relates to the theoretical signatures and gives the impact of the modes of functioning on the three residuals.

In the so-called incidence matrix or fault signature matrix of 3, 1 element indicates that the residual does repond to the failure, while 0 means that it does not [4]. At each time instant this table is used to recognize the situation. For example, if at a given time instant yhe observed signature is [1 0 1], the Hamming distance vector will be [2 0 3]; this allow to deduce, from choosing the smallest distance, that liquid failure situation has occurred.
The previous qualitative visual study showed the ability of three residues to

	free fault	solid failure	liquid failure
r_b	0	1	1
r_s	1	0	1
r_ℓ	1	1	0

Table 3: Fault signatures

easily recognize the actual operational situation. In the next section, the quantitative analysis of residues confirms this study and shows how the recognition is processed from a numerical point of view.

4.2 Generation of failure indication

With the residuals generated from the three operating models, the procedure for detecting and isolating faults reveals quite simple to implement. The principle is that the detection of amplitude variations of the residues, any sudden change can be interpreted as a change in operating mode. The standard deviation measures the dispersion of data set around its mean value, its variations may indicate the occurrence or disappearance of a failure. For a residue $r(t)$, this deviation may be calculated (with the discrete time k) over a sliding window of appropriate width N as follows:

$$\begin{cases} \sigma_{r_\lambda}(k) & = & \sqrt{\frac{1}{N-1}\sum\limits_{m=k-N+1}^{k}(r_\lambda(m)-\overline{r}_\lambda(k))^2} \\ \overline{r}_\lambda(k) & = & \frac{1}{N}\sum\limits_{m=k-N+1}^{k} r_\lambda(m) \end{cases} \tag{6}$$

This assessment is carried out on residuals (r_λ, $\lambda = b, s, \ell$) from failure-free model M_b and failure models M_s and M_ℓ. It is well known that the computation of the standard deviation may be performed using a recursive formulation. Another possibility, allowing a significant reduction of computation, is to use a exponentially weighted expression of the mean and the standard deviation of the residuals.

4.3 Failure detection by standard deviation test

Thanks to residual deviations, the detection of the operational mode and therefore failure may be performed as summarizes the algorithm 1. The principle of this algorithm is to evaluate the relationship between the calculated deviations over sliding windows of appropriate dimensions with the initial deviations (calculated in the absence of failure).

Algorithm 1 *Failure detection by standard deviation test*

1. *Initialization : Calculate the initial deviations $\sigma_{b,0}$, $\sigma_{\ell,0}$ and $\sigma_{s,0}$ from data collected in the free-failure mode.*

2. *Calculate the deviations* $\sigma_\lambda(k), \lambda = b, s, \ell$ *over sliding windows*

3. *Onset of failure: If the failure was not yet detected and that for a period of time, and if* $\sigma_b(k) \geq 2\sigma_{b,0}$*, the model* M_b *does not reflect the present situation. Moreover:*

   - *If* $\sigma_\ell(k) \leq 0.5\ \sigma_{\ell,0}$*, then the occurrence of the liquid failure is confirmed.*
   - *If* $\sigma_s(k) \leq 0.5\ \sigma_{s,0}$*, then the occurrence of the solide failure is confirmed.*

4. *Disappearance of the failure: If a failure has already been detected and that for a period of time and if :*

   - $\sigma_b(k) \leq 1.5\ \sigma_{b,0}$*,* $\sigma_\ell(k) \geq 0.75\ \sigma_{\ell,0}$ *and* $\sigma_s(k) \geq 0.75\ \sigma_{s,0}$

   then the disappearance of the failure is confirmed.

Obviously, the quantities $0.5, 0.75, 1.5$ and 2 involved in the inequality tests should be considered as parameters to be set according to the admissible level of false alarms and also to the different flight scenario. The length of the sliding window is also a parameter that must be adjusted according to tradeoff between delay time detection and insensitivity to measurement noise.

The result of failure detection by the algorithm 1 is illustrated by figures 7, 8 and 9 for the failure free case, the liquid case and the solid case respectively. As previously, the failure affects the system between 5.3 sec. and 15.3 sec and is considered at the particular frequency 1.5 Hz.

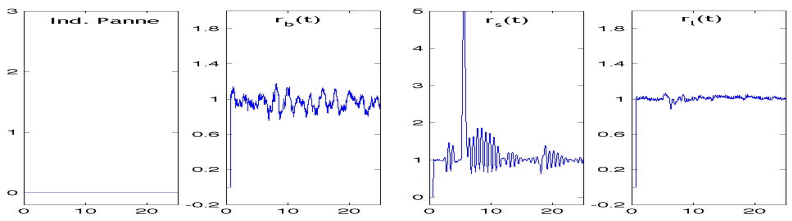

Figure 7: Result of the detection: case without failure

On each figure, the failure flag noted `Ind` is 1 if the liquid failure is detected, 2 if the solid failure is detected and 0 if no failure is detected. The quantity r_b (*resp.* r_s and r_ℓ) is the ratio between the calculated deviation on $r_b(t)$ (*resp.* $r_s(t)$ and $r_\ell(t)$) and the initial standard deviation $\sigma_{b,0}$, $\sigma_{\ell,0}$ and $\sigma_{s,0}$. This definition justifies the values taken by these ratio around the value 1 for normal operating conditions. The analysis of the different graphs, i.e. the deviation of the quantity r of its normal value 1, clearly leads to the successful conclusion of situation recognition, in all cases we have analyzed the detection of liquid

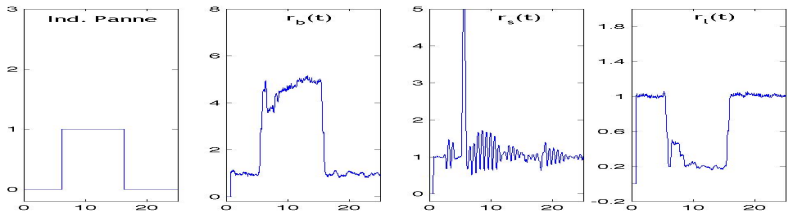

Figure 8: Result of the detection: case of liquid failure

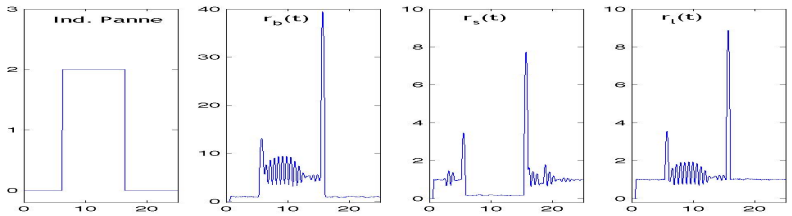

Figure 9: Result of the detection: case of solid failure

or solid failure is unambiguous. As explained in section 4.1, a fault matrix signature is used to recognize at each time instant the operating mode. Using the definition of the ratio r, table (4) has been constructed, in which element 1 indicates that the residual does repond to the failure, while 0 means that it does not

	free fault	liquid failure	solid failure
r_b	0	1	1
r_s	0	0	1
r_ℓ	0	1	0

Table 4: Fault signatures

When using noisy data, fault isolation may become difficult. For that, avoiding misisolation of the fault needs to use a specific coding of the signatures such that no degrading code is identical to a valid code. It is the case of the signatures in tables 3 and 4 which are different, but the two set of signatures are strongly isolating, according to the classical terminology [4].

4.4 Discussion on failure detection by standard deviation test

The outcomes of algorithm 1 show that the failure is detected and identified at approximately 1.0 oscillation periods after its occurrence (0.89s for the liquid failure case and 0.93 s for the solid failure case). This result is compliant with the required specifications, that is to say the detection time.

If one focuses only on the failure detection (without isolation), then only the test of standard deviation of the residual $r_b(k)$ is needed, without using the two failure models. In this case, the failure detection condition should be reduced to $\sigma_b(k) \geq 1.75\ \sigma_{b,0}$ for a period of time (algorithm 1). The different examples show that we can detect any solid and liquid failure on the frequency range $[0.5 \ldots 10.0]$ Hz even at very low amplitude (0.16 degree).

However, if the goal is to detect and isolate all failures that may appear in the control loop, the three models need to be used. Moreover, the frequency of oscillation to detect is not known a priori, only the range of variation is known.

Thus, we must consider several frequencies in the pattern of oscillation S_{def} (5) because the failure models M_s (2) and M_ℓ (3) depend on this frequency. The number of failure models described by equations (2) and (3) must be increased and therefore different frequencies of oscillations must be taken into consideration. Each failure model whose parameters are fixed is specific to a particular solid or liquid failure (of type (5)). With the principle used by the algorithm 1, any solid and liquid failure characterized by a frequency in $[0.5 \ldots 10.0]\ Hz$ and an amplitude in $[0.5 \ldots 1.0]\ deg$ can be detected and isolated for many flight scenarios. This procedure has been developed and successfully tested on different flight situations.

However, to reduce the number of failure models, another approach is to use a correlation test that is developed in the next section.

5 Fault detection by correlation test

The dysfunction models (2 and 3) allow to study the behavior of the system in the presence of a failure, liquid or solid. In the simulation of dysfunction models, by forcing the command to zero, the impact of the failure on the output can be directly identified and estimated. In this way, patterns of failures can be generated offline to be compared to the residue $r_b(t)$ or output $x(t)$ to detect and isolate the failure.
Figure 10 shows the procedure to be implemented. The first residue $r_b(t)$, generated by the model M_b has already been defined. Signals $f_i(t)$ correspond to failures (5) characterized by some specific frequencies (0.5 Hz, 1.5 Hz, 7 Hz for example) whose effect is assessed based on the failure models M_ℓ thus generating signatures $x_{Li}(t)$ specific to each of these frequencies. It is important to note that $x_{Li}(t)$ reflect only the influence of the failure, since the input u is not applied to the models M_ℓ. Moreover, by construction, residual $r_b(t)$ is also insensitive to $u(t)$ but reflect the influence of the fault f if it is present.

Such frequencies are called "selected" because this work aims at detecting and isolating the failures of these frequencies. These signatures are then compared (by correlation over sliding windows) to the previously evaluated residue $r_b(t)$ or output $x(t)$. This principle applies to liquid failure with model M_ℓ as indicated on figure 10. The same procedure applies for solid failure with model M_ℓ.

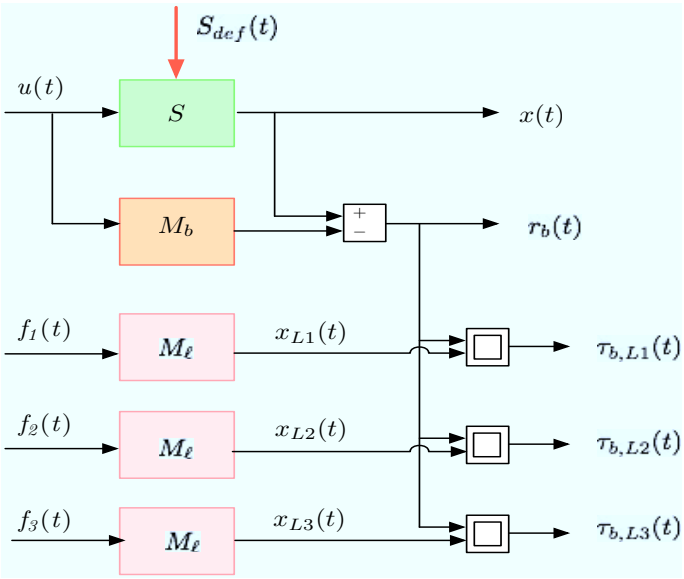

Figure 10: Generation of residues for correlation test. Case of liquid failure

5.1 Pattern generation

In this subsection patterns at 0.5 Hz, 1.5 Hz and 7.0 Hz are generated from models M_s and M_ℓ by putting the command to zero. As the correlation test does not distinguish the amplitudes of sinusoidal signals, these patterns are generated so that they correspond with the oscillation of 0.75 deg. Each pattern is a sequence of length equal to two periods of the failure of the same frequency. The objective is to detect and to isolate the three failures $f(t) = 0.75sin(2\pi f.t)$ for the frequencies 0.5 Hz, 1.5 Hz and 7.0 Hz.

5.1.1 Patterns of liquid failures

For the liquid failures, three following patterns are generated (table 5) with a sampling period of 0.01 sec.

These three patterns x_{L1}, x_{L2} and x_{L3} are presented in figure 11. They will be used in a correlation test with the signal $r_b(t)$ defined previously by $r_b(t) = x(t) - x_b(t)$.

Pattern	Sequence	Frequency
x_{L1}	400 samples	0.5 Hz.
x_{L2}	134 samples	1.5 Hz.
x_{L3}	29 samples	7.0 Hz.

Table 5: Liquid failure patterns

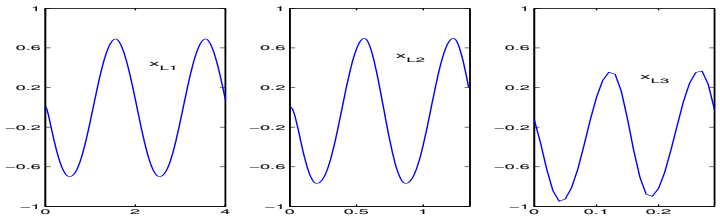

Figure 11: Patterns x_{L1}, x_{L2} and x_{L3}

As explained before, the patterns x_{L1}, x_{L2} and x_{L3} are the direct impacts of liquid failures (without the influence of the command $u(t)$) on the output of the system and they are comparable in some way with the residue $r_b(t)$ under the presence of a failure. Indeed, the difference $x(t) - x_b(t)$ reflects the impact of the failure on the output since the effect of the command $u(t)$ on $x(t)$ and $x_b(t)$ is canceled by difference.

5.1.2 Patterns of solid failures

For the solid failures, three following patterns are generated (table 6). These

Pattern	Sequence	Frequency
x_{S1}	400 samples	0.5 Hz.
x_{S2}	134 samples	1.5 Hz.
x_{S3}	29 samples	7.0 Hz.

Table 6: Solid failure patterns

three patterns x_{S1}, x_{S2} and x_{S3} are presented in figure 12. They are analyzed by correlation test with the actual output $x(t)$.

5.2 Failure indicator generation and fault detection by correlation test

The correlation between two or more variables, such as r_b and x_{Li} is the intensity of the relation that may exist between these variables. A measure of this correlation is obtained by the calculation of the linear correlation coefficient.

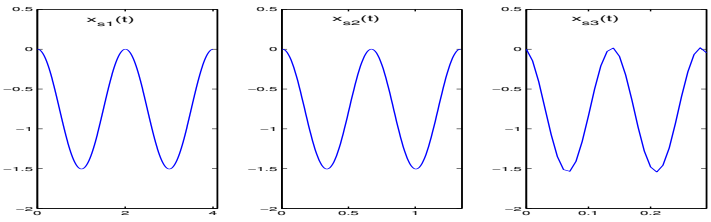

Figure 12: Patterns x_{S1}, x_{S2} and x_{S3}

The linear correlation coefficient between two variables r_b and x_{Li} is noted by $\tau_{b,Li}$.
With the correlation test, FD can be performed as summarized in Algorithm 2. The principle of this algorithm is to compute the linear correlation coefficients over a sliding window, on the one hand between the residue $r_b(t)$ with signals x_{L1}, x_{L2} and x_{L3} which represent liquid failures; on the other hand between the output $x(t)$ with signals x_{S1}, x_{S2} and x_{S3} which represent solid failures. If one of these coefficients calculated over a sliding window exceeds a threshold a certain number of times within a limited time, a failure is detected.

Algorithm 2 *Fault detection by correlation test*

1. *Initialization :*
   - *Read the patterns for the liquid failure* x_{L1}, x_{L2} *and* x_{L3}
   - *Read the patterns for the solid failure*x_{S1}, x_{S2} *and* x_{S3}
   - *Define the vector of pattern sizes* $p = [400 \quad 134 \quad 29]$
   - *Chose one threshold as for example* $V_s = 0.6$.
2. *Perform calculations of linear correlation coefficients for each* k^{th} *sampling step:*
   - *Calculate the correlation for liquide failure* $\tau_{r_{b(k-p(i)+1:k)},x_{Li}}$ *for* $i = 1, 2, 3$.
   - *Calculate the correlation for solid failure* $\tau_{x_{(k-p(i)+1:k)},x_{Si}}$ *for* $i = 1, 2, 3$.
3. *Evaluate the linear correlation coefficients by counting exceedances:*
   - *If a correlation coefficient is greater than* V_s *or smaller than* $-V_s$, *the number of so-called overruns associated with this coefficient is increased by one unit.*
   - *If no exceedance were observed within a limited time, the number of overruns is set to zero.*
4. *Onset of failure: If the failure has not yet been detected and if one of the overruns is greater than or equal to 4; then:*

- *The onset of failure is confirmed.*
- *The nature of the failure (liquid or solid) as well as its frequency are indicated by the pattern x_{Li} or x_{Si} whose number of exceedances was observed with its correlation coefficient. If it is a pattern x_{Li}, the failure is liquid; if it is a pattern x_{Si}, the failure is solid. The value of i (1, 2 or 3) indicates the frequency of the failure.*

5. *Disappearance of the failure: If a failure has already been detected and no exceedance was observed within a limited time; then*
   - *the failure is declared to have disappeared.*

The correlation coefficients calculated during the time are shown first in figure 13 for the case without failure. The result of failure detection by the algorithm 2 is shown in figures 14, 15 and 16. Figure 14 (*resp.* 15 and 16) represents the result obtained with the liquid failure of 0.5 Hz frequency (*resp.* the liquid failure of 1.5 Hz frequency and with the solid failure of 7.0 Hz frequency). Failures are simulated between 5.3 and 15.3 seconds.

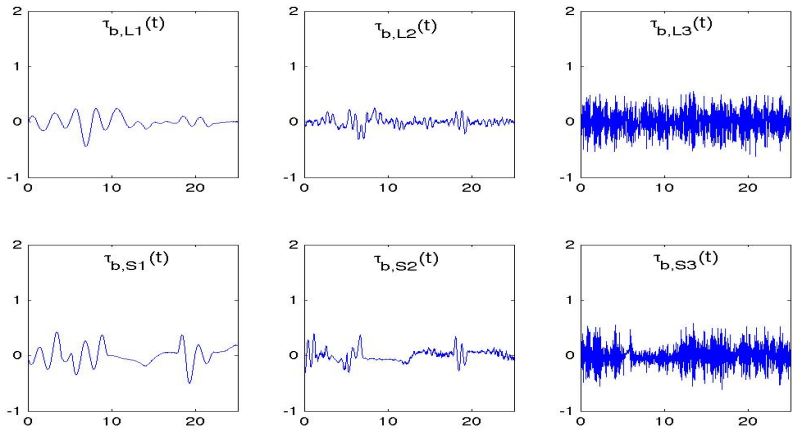

Figure 13: Calculated correlation coefficients : case without failure

The first column represents the correlation coefficient which led to the failure detection ($\tau_{r_b,x_{L1}}$, $\tau_{r_b,x_{L2}}$ and $\tau_{x,x_{S3}}$ respectively). The indicator of nature of the failure is noted by `Nat` in the second column. If `Nat` = 1, a liquid failure is detected, if `Nat` = 2, a solid failure is detected, and `Nat` = 0 is used in the free-failure case. The frequency of the failure is indicated in the third column. With this method, the detection and isolation of failure can be performed in less than three periods of the failure, which is in fact compliant with the required

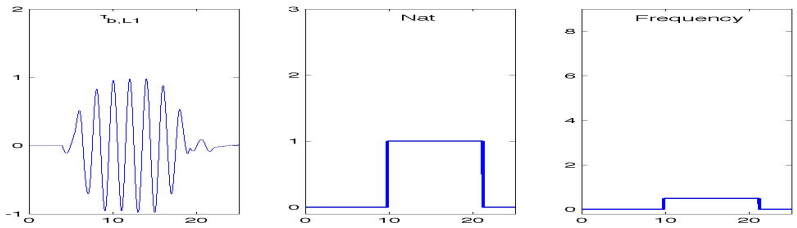

Figure 14: Result of detection : liquid failure of 0.5 Hz frequency

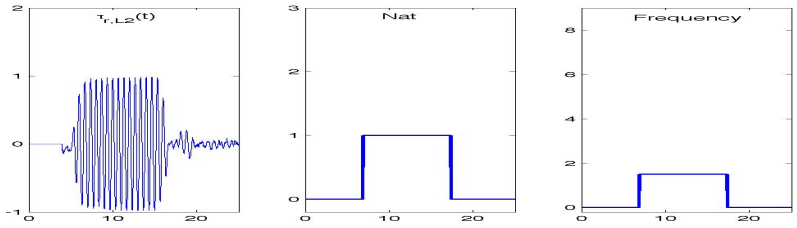

Figure 15: Result of detection : liquid failure of 1.5 Hz frequency

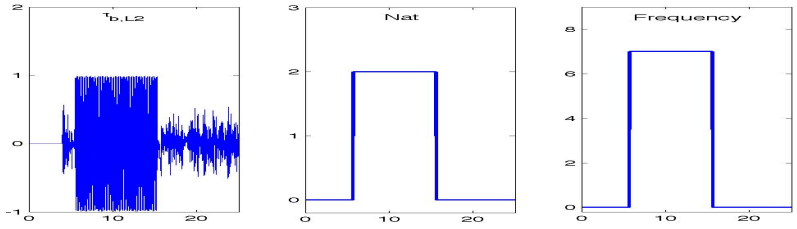

Figure 16: Result of detection : solid failure of 7.0 Hz frequency

specifications. More precisely, frequency 0.5 Hz corresponds to period of 2 sec. On figure 14, the detection et the recognition of the failure is performed at 10 sec., i.e. with a delay of 4.7 sec. which is less that three periods of the failure. The same analysis should be done for the two other cases.

5.3 Discussion on the failure detection by correlation test

Failure detection by correlation test has reduced significantly the number of failure models compared to deviation test. In fact, boarding only failure-free model in flight control computer to generate the residue $r_b(t)$ is sufficient. All the pattern describing liquid and solid failures are generated in advance and stored and thus the on-line computation task is easy to perform. Different treated flight

scenarios show that any solid and liquid failure characterized by frequencies in the frequency range $[0.5 \dots 10.0]\ Hz$, even at low amplitude ($0.16\ deg$) can be detected and isolated. However, this analysis does not estimate the amplitude of the failure.

It should be noted that, in its current version, the algorithm 2 uses six correlation tests at every step of simulation (two types of default, three selected frequencies). Although the calculations are simple and need basic operators, it is possible to substantially reduce the computational load :

- The patterns x_{L1}, x_{L2}, x_{L3}, x_{S1}, x_{S2} and x_{S3} are determined by the type of failure. Their means and standard deviations over a window can be calculated offline and stored.
- Means, standard deviations of the output $x(t)$ and the residue $r_b(t)$ calculated over a window can be performed recursively when moving a step time of the observation window.
- The covariance, and consequently the correlation, between a reference pattern and a signal $x(t)$ or $r_b(t)$ over a window can also be calculated in recursive way.

These recurrences are easy to establish, so the correlation tests can be carried out with a reasonable computational load.

6 Conclusion

This paper addresses the problem of detecting the oscillatory failure in the control system of a control surface of a civil aircraft. Two fault detection methods are proposed, based on a simplified model validated regarding the nonlinear models usually used. Any solid and liquid failure in the frequency range $[0.5 \dots 10.0]\ Hz$ can be detected by standard deviation test, as well as any solid and liquid failure of selected frequencies by correlation test. Both methods have been successfully tested for a variety of flight scenarios, even with failures of low amplitude (0.16 degree). Future works will consist in extending these methods to other control surfaces (rudder or elevator), by trying to reduce the complexity as well as the number of failure models. The improvement of the robustness of the correlation test for the failures of frequencies neighboring the selected ones is also to be considered.

Acknowledgement. The authors would like to thank the French Research Foundation for Aviation and Space, for its support to the SIRASAS project.

References

[1] H. Alwi and C. Edwards. Oscillatory failure case detection for aircraft using an adaptive sliding mode differentiator scheme. In *American Control Conference (ACC), 2011*, pages 1384–1389, 2011.

[2] J. Cieslak, D. Efimov, A. Zolghadri, D. Henry, and P. Goupil. Oscillatory Failure Case Detection for Aircraft using Non Homogeneous Differentiator in Noisy Environment. In *2nd CEAS Specialist Conference on Guidance, Navigation & Control*, Delft, Netherlands, 2013.

[3] P. Dash, R. Jena, G. Panda, and A. Routray. An extended complex Kalman filter for frequency measurement of distorted signals. *IEEE Transactions on Instrumentation and Measurement*, 49(4):746–753, 2000.

[4] J. Gertler. Analytical redundancy methods in fault detection and isolation ; survey and analysis. In *IFAC International Symposium on Fault Detection, Supervision and Safety for Technical Processes*, volume 1, pages 9–21, 1991.

[5] P. Goupil. Oscillatory failure case detection in the a380 electrical flight control system by analytical redundancy. *Control Engineering Practice*, 18(9):1110–1119, 2010.

[6] Q. P. He, J. Wang, M. Pottmann, and S. J. Qin. A curve fitting method for detecting valve stiction in oscillating control loops. *Industrial & engineering chemistry research*, 46(13):4549–4560, 2007.

[7] G. J. Jeram and J. Prasad. Fuzzy logic detector for aircraft pilot coupling and pilot induced oscillation. In *the 59th American Helicopter Society Annual Forum*, volume 59, pages 1204–1211, 2003.

[8] K.-S. Kim, K.-J. Lee, and Y. Kim. Reconfigurable flight control system design using direct adaptive method. *Journal of Guidance, Control, and Dynamics*, 26(4):543–550, 2003.

[9] L. Lavigne, A. Zolghadri, P. Goupil, and P. Simon. Robust and early detection of oscillatory failure case for new generation airbus aircraft. In *the AIAA Guidance, Navigation and Control Conference and Exhibit*, 2008.

[10] L. Marton and D. Ossmann. Energetic approach for control surface disconnection fault detection in hydraulic aircraft actuators. In *IFAC International Symposium on Fault Detection, Supervision and Safety of Technical Processes*, volume 8, pages 1149–1154, 2012.

[11] D. Mitchell and D. Klyde. *Recommended Practices for Exposing Pilot-Induced Oscillations or Tendencies in the Development Process*. American Institute of Aeronautics and Astronautics, 2004.

[12] M. Sifi, L. Lavigne, F. Cazaurang, and P. Goupil. Oscillatory failure detection in Flight Control System of civil aircraft: EHA actuator servo loop case study. In *5th International Conference on Recent Advances in Aerospace Actuation Systems and Components (R3ASC'12)*, 2012.

[13] X. Sun, R. J. Patton, and P. Goupil. Robust adaptive fault estimation for a commercial aircraft oscillatory fault scenario. In *UKACC International Conference on Control (CONTROL)*, pages 595–600, 2012.

[14] D.-H. Trinh, B. Marx, P. Goupil, and J. Ragot. Design of a soft sensor for the oscillatory failure detection in the flight control system of a civil aircraft. In *2010 IEEE International Symposium on Industrial Electronics (ISIE)*, pages 2061–2066. IEEE, 2010.

[15] A. Varga and D. Ossmann. LPV-model based identification approach of oscillatory failure cases. In *IFAC International Symposium on Fault Detection, Supervision and Safety of Technical Processes*, volume 8, pages 1347–1352, 2012.